An improved bias correction for SSMIS

Anna Booton, William Bell, Nigel Atkinson
Met Office, FitzRoy Road, Exeter, UK

Abstract

The currently operational SSMIS instruments are subject to complex orbital biases, resulting from calibration anomalies including reflector emissions and solar intrusions. To date, physically based correction techniques have only been partially successful in correcting the measured radiances. Consequently, due to the difficulty in dealing with these biases, the full potential of SSMIS to provide high quality imager data, and sounding data throughout the troposphere to mesosphere, has yet to be realised.

An improved bias correction scheme is introduced for SSMIS. The scheme adopts a Fourier-based approach, whereby a compliment of bias predictors comprised of Fourier components are used to parameterise the bias along the satellite track. When this compliment is extended to include higher order Fourier terms the correction is able to mitigate the orbital biases effectively.

The characterisation of the orbital biases are presented for data from the F-18 satellite. The anticipated effectiveness of the scheme is assessed through a toy model.

1. Introduction

The three Special Sensor Microwave Imager Sounder (SSMIS) instruments currently operating provide temperature and humidity soundings as well as imager data, measuring radiances from the surface into the mesosphere. The instruments are conical scanning radiometers that operate by reflecting upwelling radiation from a large rotating mirror into feedhorns. Unfortunately the open design of the conical scanners has led to several calibration anomalies such as reflector emissivity imperfections and warm load solar intrusions. Consequently the measured radiances are subject to complex orbital biases that are difficult to correct.

To date, attempts to correct the biases using physically based corrections have only been partially successful in reducing the amplitude of the residual biases from around 1 K to 0.3 K. In the last few years it has become evident that the requirements on any bias correction scheme are increasingly demanding. In order to avoid degradation to numerical weather prediction (NWP) analysis and forecast accuracy, it is a reasonable rule-of-thumb to demand that local residual biases after bias correction should ideally be at least an order of magnitude less than the geophysical signals being corrected. For the lower atmospheric temperature sounding channels it is known that the geophysical signals are in the range 50-100mK, and therefore the bias correction scheme should leave residual biases of 5-10 mK. An improved bias correction scheme is therefore explored that exploits the NWP model based bias prediction method proposed by Harris and Kelly (2001), providing an additional, complementary approach to the physically based techniques currently used for SSMIS.

Calibration anomalies manifested as complex systematic biases can be elucidated through comparisons between observed brightness temperatures (O) and those calculated from NWP model backgrounds (B). Furthermore, corrected brightness temperatures (C) can be used to assess the effectiveness of any bias correction scheme. Such 'C-B' analysis of SSMIS temperature sounding channels, for which the NWP model background equivalent is highly accurate clearly reveals an "ascending/descending" structure, or orbital biases, for the SSMIS instruments. As shown in Figure 1, despite the application of both pre-processing and bias correction, the descending passes remain significantly cooler, by 0.5 K, than the ascending. Although particularly pronounced in the F-18 data, similar signals are present in both F-16 and F-17 instruments.

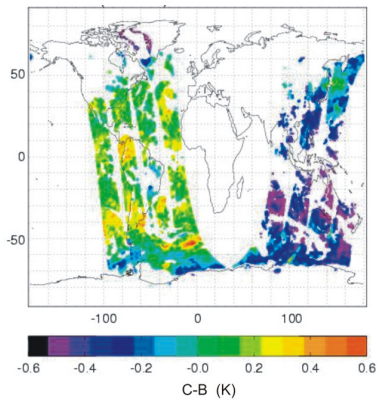

Figure 1: (C-B) brightness temperature departures for F-18 SSMIS 55 GHz channel (Ch 5) shows that systematic bias remains in the data despite physically based bias corrections already being applied.

2. An ascending/descending bias predictor

In order to compensate for the ascending/descending bias, a new bias predictor was developed whereby application of a cosinusoidal predictor was found to effectively reduce the departures. When implemented, the predictor is scaled accordingly and subtracted from the observed brightness temperatures, thus removing the ascending/descending bias. The correction is given by:

$$\Delta T_B(L) = \beta . d \cos(L + \theta) \qquad (1)$$

where the predictor, $d\cos(L+\theta)$, depends on the direction of the satellite pass, d such that $d = +1$ during the ascending pass and $d = -1$ if desending, as well as the latitude, L, of the observation and a phase shift, θ, offsetting the correction from the equator. It is scaled using β, the bias coefficient. When applied, the predictor was found to be globally effective, reducing departures from ~1 K to approximately ±100 mK, as shown in Figure 2. However it was only partially successful, as, unable to fully capture the complex structure, localised biases remained. Additionally, the effectiveness of the correction was found to lessen with time due to a seasonal dependency causing the magnitude and the position of the maximum bias to vary throughout the season. Unfortunately, in order to maintain benefit from utilization of the correction, it is then necessary to regularly (~monthly) update the bias parameters, β and θ.

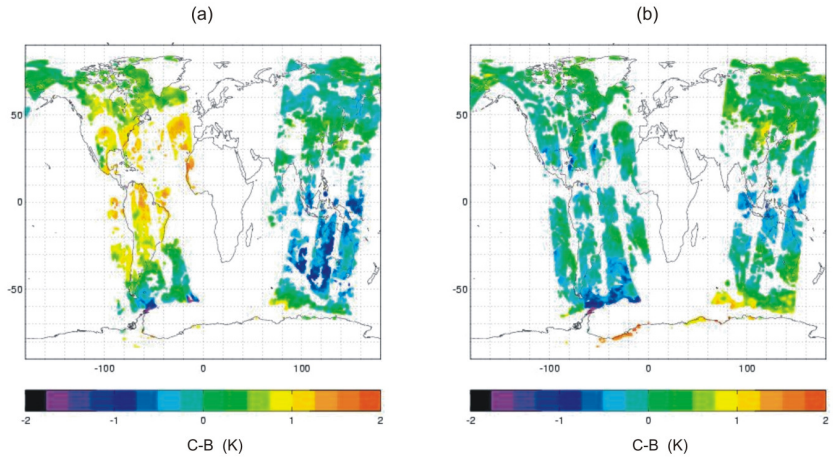

Figure 2: (C-B) brightness temperature departure maps for F-18 SSMIS 60.8 GHz channel (Ch 24) data, pre processed via the UPP[1] and with Met Office standard NWP bias correction (a) without and (b) with the inclusion of the additional "ascending/descending" predictor. Some localised biases remain, such as over Indonesia, but overall the residual biases are significantly reduced.

3. An improved orbital bias predictor: a Fourier approach

An orbital bias predictor should be a periodic function, representative of the cyclic nature of the orbital bias, thus a Fourier series expansion is ideal. An improved correction scheme was therefore developed of the following form,

$$\Delta \mathrm{T_B}(\phi) = \sum_{i=0}^{N} a_i \cos(i\phi) + b_i \sin(i\phi) \qquad (2)$$

This scheme comprises a set of N cosinusoidal predictors, $\cos(i\Phi)$, and their associated coefficients, a_i, and a set of N sinusoidal predictors, $\sin(i\Phi)$, and coefficients, b_i. The inclusion of higher order Fourier terms provides an enhanced capability for fitting to, and hence correcting, complex bias structures. Secondly, deriving the correction as a function of the satellite's "along-track" or "orbital" angle Φ, as depicted in Figure 3, facilitates the use of a smooth and continuous periodic predictor. Since Φ is determined relative to the position of the sun, the seasonal biases previously observed should be reduced, and the predictor's stability improved. Furthermore, equation 2 is easily adapted to the Harris and Kelly scheme in which the bias correction is obtained as,

$$\Delta \mathrm{T_B}(\hat{\mathrm{x}}) = \sum_{i=1}^{M} \beta_i \mathrm{P_i}(\hat{\mathrm{x}}) \qquad (3)$$

where there are M bias predictors, P_i , and their associated regression bias coefficients, β_i. $\hat{x}$ represents a state vector incorporating model and observation related variables. Hence the orbital bias correction of equation 2 may be implemented within the Met Office's bias correction system.

[1] The SSMIS Unified Pre-Processor (UPP) applies SSMIS specific, physically based bias correction (Bell *et al.*, 2008). The SSMIS UPP Averaging Module is used for averaging the data (NWPSAF, 2010).

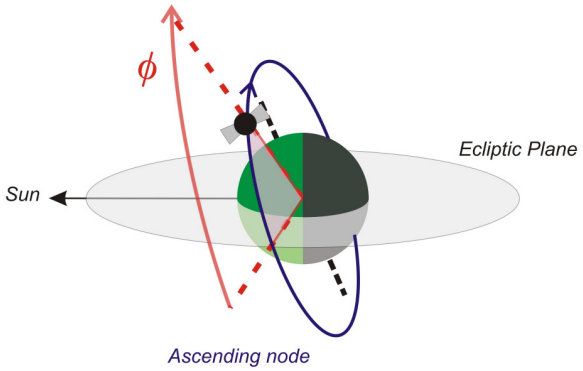

Figure 3: Sketch of the satellite orbiting the earth, with the satellite making an angle Φ about the orbital track, relative to the intersection of the satellite's ascending node with the ecliptic plane.

3.1. Implementing the predictor

A toy model representative of the variational bias correction (VarBC) data assimilation system that the Met Office is currently implementing, was developed to investigate the performance of the Fourier based correction scheme. In such a scheme the changing nature of the bias is accommodated by employing bias coefficients that are updated regularly. In this case, the residual biases (O-B) were corrected at each analysis cycle (i.e. every 6 hours) using coefficients, β', derived from the previous cycle; then updated coefficients β were computed. The update was calculated by minimising the cost function:

$$\mathrm{J}(\beta) = \frac{\left(\sum_{k=1}^{all\ obs} \left[(\mathrm{O\text{-}B})(\phi_k) - \sum_{i=1}^{M} \beta_i \mathrm{P}_i(\phi_k) \right] \right)^2}{\sigma_O{}^2} + \frac{\left(\sum_{i=1}^{M} \left(\beta_i - \beta_i' \right) \right)^2}{\sigma_B{}^2} \qquad (4)$$

Here the first term is a measure of the current observations' (*all obs*) contributions whilst the second is a measure of prior contribution. This latter term, the 'inertia constraint' (Auligne, 2007) determines how much β_i adapts at each assimilation cycle. The 'inertia' is in turn controlled by the weighting terms σ_O and σ_B.

Substituting to include the Fourier series predictor (equation 2) in equation 4 gives:

$$\mathrm{J}(a,b) = \frac{\left(\sum_{k=1}^{all\ obs} \left[(\mathrm{O\text{-}B})(\phi_k) - \sum_{i=0}^{N} a_i \cos(i\phi_k) + b_i \sin(i\phi_k) \right] \right)^2}{\sigma_O{}^2} + \frac{\left(\sum_{i=0}^{N} \left(a_i - a_i' \right) + \left(b_i - b_i' \right) \right)^2}{\sigma_B{}^2} \qquad (5)$$

In order to implement this function, the number of predictors, N, must be chosen and the weightings optimized. The weighting, σ_O is determined by the number of observations presented to the assimilation cycle (for a given instrument channel). Therefore, the relative weighting, σ_O / σ_B, ratio was optimized for each channel accordingly, and was assumed to remain constant throughout the test period.

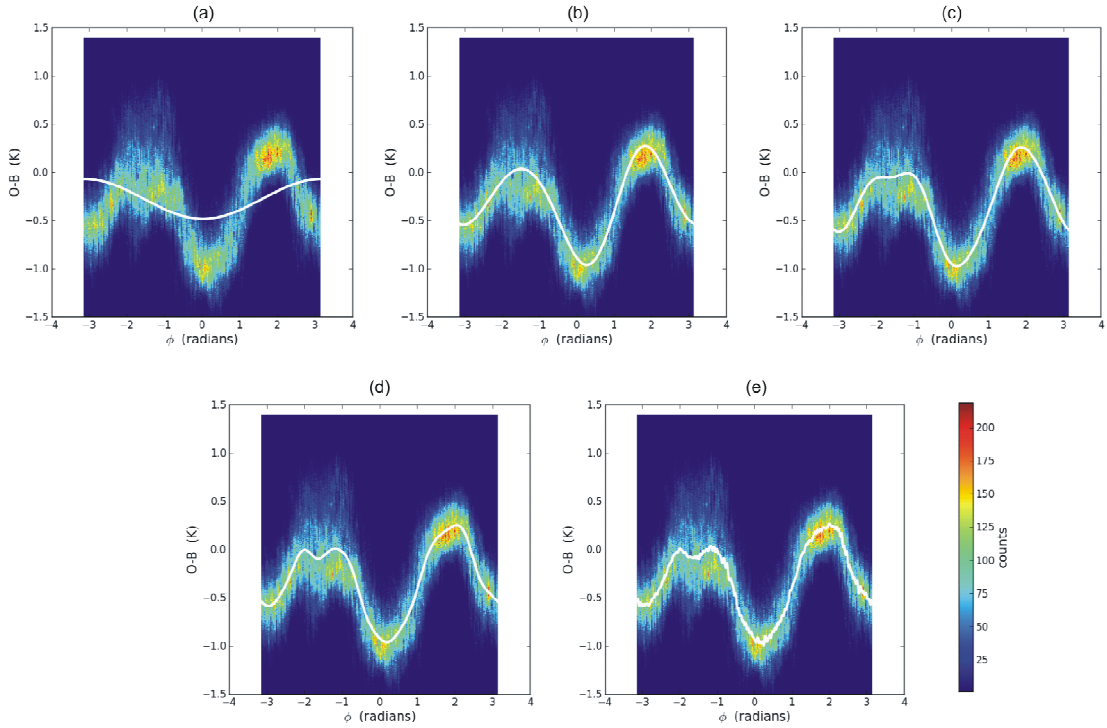

Figure 4: 2*D* histograms of (O-B) brightness temperature departure plotted w.r.t Φ for data accumulated for F-18 SSMIS 57 GHz channel (Ch 6), over 13 cycles at the autumn equinox, from QU00 Sep 19th 2013. Fourier series are over-plotted in white, as calculated for N=1, 3, 5, 10, and 98 in (a)-(e) respectively.

The number of bias predictors required to adequately capture the structure of the residual bias was ascertained prior to running the toy model. F-18 SSMIS O-B brightness temperature data was collected with respect to Φ over a three day period (13 cycles) and Fourier series were fitted to it. When the data is presented as a 2*D* histogram of brightness temperature departures versus Φ, as in Figure 4, the nature of the orbital bias is elucidated. In this case the bias associated with the satellite's ascending pass ($-1.5 < \Phi < +1.5$ rad) has a minimum temperature difference of -1 K, whilst the descending pass is approximately 1 K warmer. This is most clearly depicted in Figure 4 (a) as the nodes of the fitted co-sinusoidal Fourier series (N=1) corresponds to the satellite's ascending/descending transitions. (This fit is similar to that obtained using the original "ascending/descending" predictor although this generates a squared co-sinusoidal fit w.r.t Φ). This fit struggles to capture the fundamental structure of the bias. However, as the number of Fourier components is increased the fit is improved (Figure 4 (a - d)), although at very high orders of N, such as $N = 98$ (Figure 4 (e)), the structure becomes over-fitted. The Fourier series comprised of 10 components (N=5) was deemed to provide a good fit to the overall structure, whilst minimising the computation required. Consequently a predictor scheme utilizing 10 bias predictors was selected.

4. Results from the toy model

The toy model with a 10 component Fourier series predictor and optimally tuned weightings ($\sigma_O = 1$, $\sigma_B = 390$), was presented with four assimilation cycles of SSMIS data (F-18, 57 GHz). At each iteration the Fourier series correction (of equation 2) was over-plotted on the (O-B) departures as in Figure 5 (a), and the envelope of these variational fits is emphasised in white. The deviation between the fits is most notable in the region of $\Phi \sim -2$ rad where the envelope is widest, and overall the envelope is seen to capture the orbital bias structure well. Consequently the corrected departures shown in Figure 5 (b) are reduced to near zero, indicating that the correction was effective in mitigating the residual biases.

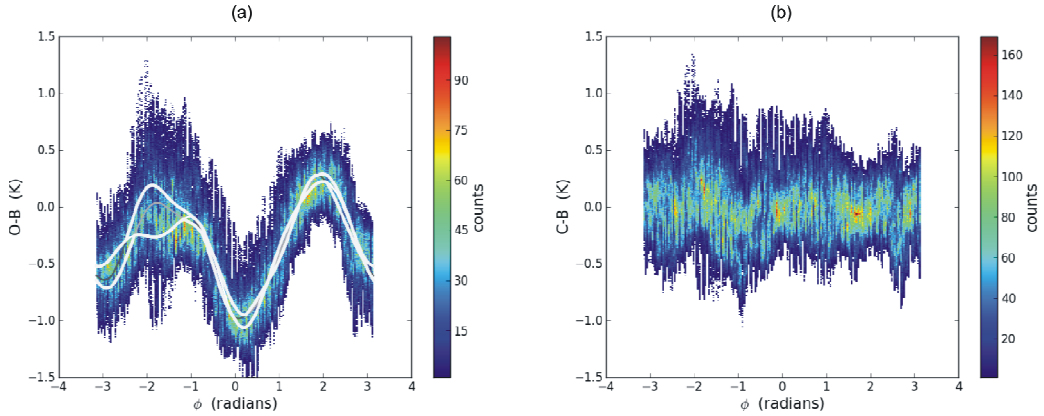

Figure 5: 2*D* histograms of (a) (O-B) brightness temperature departures plotted w.r.t Φ for data accumulated for F-18 SSMIS 57 GHz channel (Ch 6), over 4 cycles from Sep 20th 2013. Fourier series corrections ΔT_B are over-plotted with their envelope in white. (b) (C-B) brightness temperature departures as obtained from the variational toy model scheme.

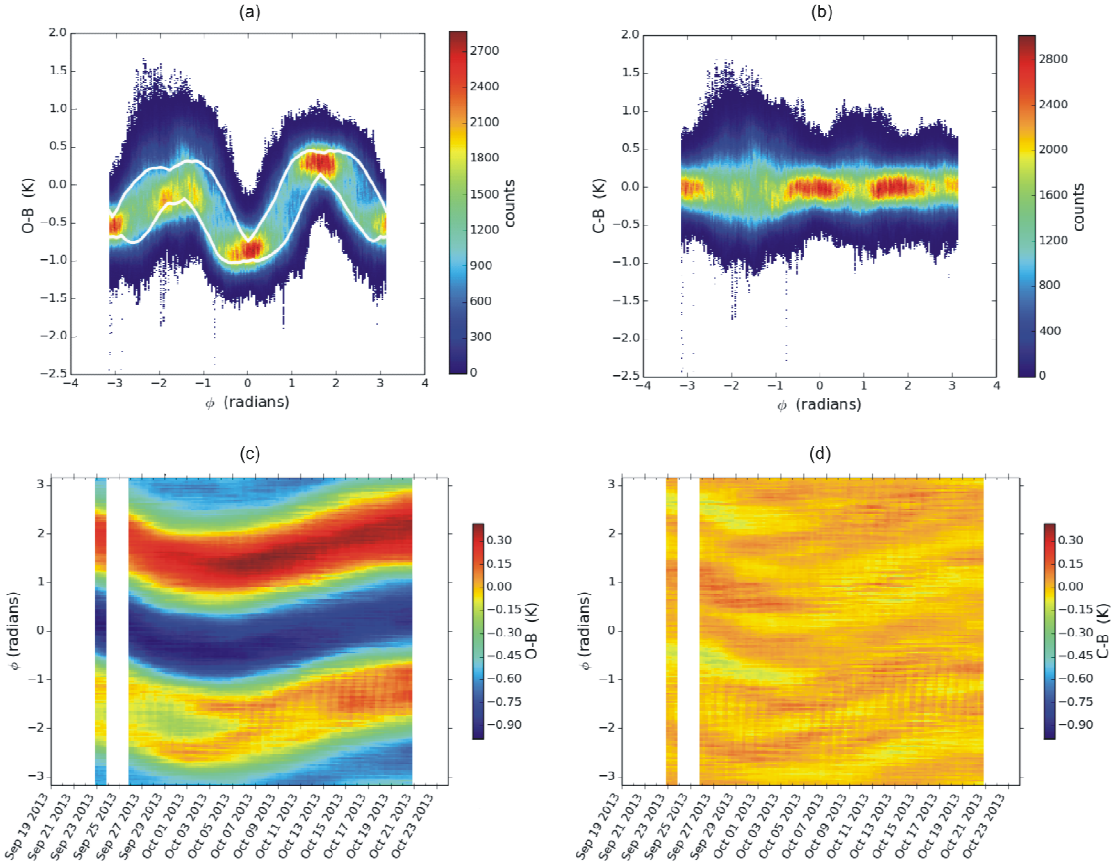

Figure 6: (a) 2*D* histograms of (O-B) brightness temperature departures plotted w.r.t Φ for data accumulated for F-18 SSMIS 57 GHz channel (Ch 6), over 115 cycles (30 days) from Sep 20th – Oct 20th 2013. The envelope of the Fourier series corrections, ΔT_B, are over-plotted in white. (b) 2D histograms of (C-B) brightness temperature departures as obtained from the variational toy model scheme. (c) and (d) Rolling mean brightness temperature departures plotted versus Φ, for data accumulated from the previous 10 cycles (60 hours), for (c) (O-B) and (d) (C-B) data.

The toy model was subsequently run for a longer, thirty day period (115 cycles). The (O-B) brightness temperature departure histograms presented in Figure 6 (a) also with the envelope of the applied (115) corrections over-plotted. Over this period the envelope is seen to fit the general bias structure very well. Accordingly, the corrected departures shown in Figure 6 (b) exhibit little structure with respect to Φ, indicative that residual biases are successful reduced.

Further analysis of the thirty day experiment demonstrates that the orbital bias structure has evolved throughout the period. In Figure 6 (c) and (d) rolling mean brightness temperature departures are plotted versus Φ, from statistics accumulated from 10 assimilation cycles (60 hours). When presented as a time series, the structure of the residual bias in Figure 6 (c) is seen to evolve smoothly during the month. The corrected bias departures, Figure 6 (d), do not exhibit this, indicating that the variational correction has also evolved in time. Although some small localised bias remains, the majority of the remaining bias is 35 mK (quantified as the mean absolute difference of the departures in Figure 6(d)) and the standard deviation is ~200 - 300 mK over the majority of the orbit. Further improvements were gained by implementing screening of observations within the toy model. Using the Met Office's current quality control to primarily select cloud free 'good' observations resulted in the standard deviation being reduced to ~100 - 200 mK.

Similar analysis was carried out for a surface sensitive channel (F-18, 37V GHz) data utilizing sea, cloud-free observations. Unlike the results for the 57 GHz channel presented in Figure 6 (a), the imager channel is relatively insensitive to the strong orbital biases, as characterised by the

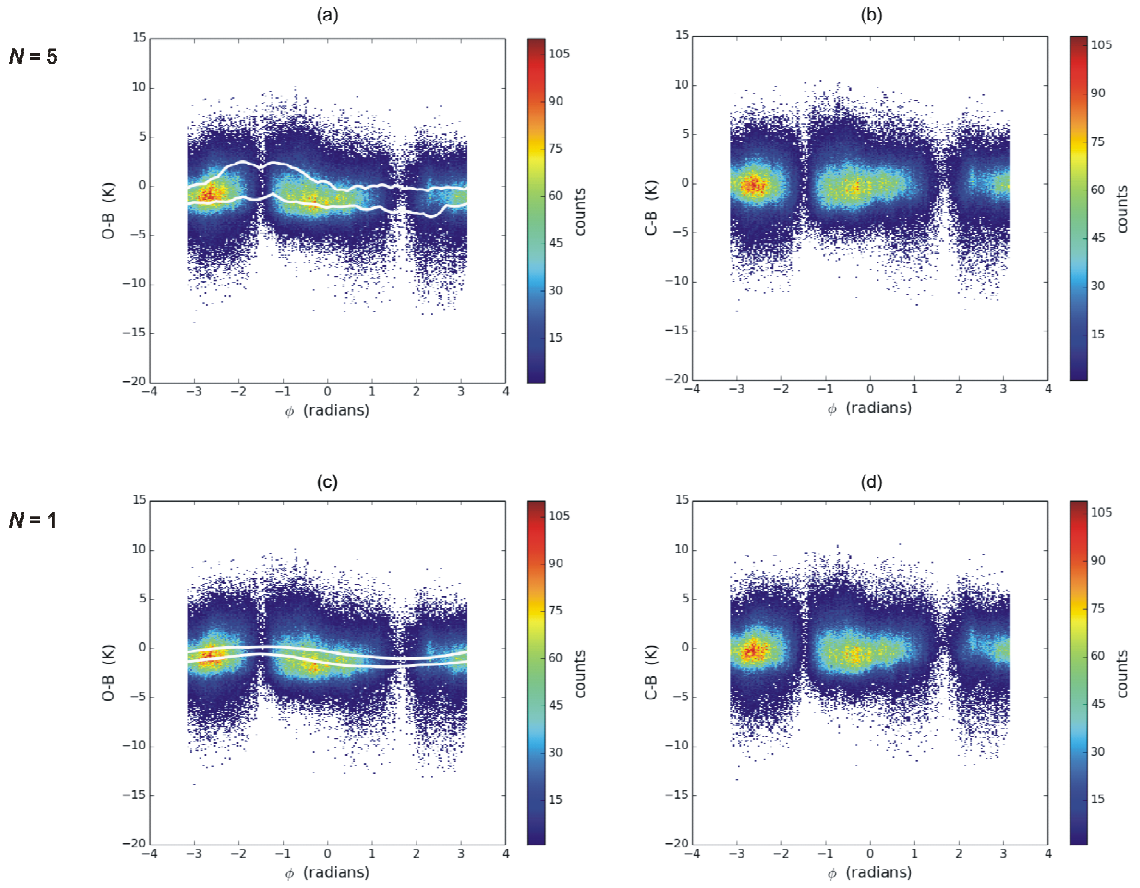

Figure 7: (a,c) 2*D* histograms of (O-B) brightness temperature departures plotted w.r.t Φ for screened data accumulated for F-18 SSMIS 37V GHz channel (Ch 16), over 115 cycles (30 days) from Sep 20th – Oct 20th 2013. The envelope of the (a) 10 component and (c) 2 component Fourier series corrections, ΔT_B, are over-plotted in white. (b,d) 2*D* histograms of (C-B) brightness temperature departures as obtained from the variational toy model scheme using a (b) 10 component correction and (d) 2 component correction.

relatively featureless (O-B) brightness temperature histograms presented in Figure 7 (a). This is partly due to the lower reflector emissivity at lower frequencies, and partly due to the contribution due to the larger background error in the humidity sensitive channels. The correction does still provide benefit, with the (C-B) corrected brightness temperature departures (Figure 7(b)) being reduced to near zero as before. However, given the lack of structure in the orbital bias, a Fourier series correction comprised of fewer components is adequate. In Figure 7 (c - d), the results from a correction comprised of just two components (N=1) are presented. Assessing the envelope of the Fourier fits (Figure 7(a)) highlights that this simpler function smoothly fits the orbital bias structure, whilst the (C-B) departures indicate the correction to be giving slight benefit.

5. Conclusions

In conclusion, the SSMIS instruments exhibit complex orbital biases even after physical corrections have been applied. A new orbital bias scheme is under development using a Fourier series based predictor. Investigations with a variational bias correction toy model show that implementing a predictor comprised of 10 components, or less components for surface sensitive channels, and tuned weightings enables the residual orbital bias to be effectively mitigated. The temperature sounding channel biases *post* correction are reduced to <50 mK in amplitude throughout the month period, (results shown for a 30 day test with F-18, 57 GHz (Ch 6) data). Orbital biases were mitigated in the surface sensitive channels by analysing bias corrections from sea-clear screened observations (results for F-18, 37V GHz (Ch 16) data). Results are consistent between instruments on F16, F17 and F18. Further steps include implementing in the Met Office's operational system.

6. References

Auligne, T, McNally, AP, Dee, DP, (2007) Adaptive bias correction for satellite data in a numerical weather prediction system. Quarterly Journal of the Royal Meteorological Society, **133**, pp 631-642

Bell, W, Candy, B, Atkinson, N, Hilton, F, Baker, N, Bormann, N, Kelly, G, Kazumori, M, Campbell, WF, Swadley, SD, (2008) The assimilation of SSMIS radiances in numerical weather prediction models. IEEE Transactions on Geoscience and Remote Sensing, **46**, 4, pp 884-900

Harris, BA, and Kelly, G, (2001) A satellite radiance-bias correction scheme for data assimilation. Quarterly Journal of the Royal Meteorological Society, **127**, pp 1453-1468

NWPSAF, (2010) SSMIS UPP Averaging Module Technical Description, NWPSAF-MO-UD-025, v1.0